The 8th European Congress on Computational Methods in Applied Sciences and Engineering
ECCOMAS Congress 2022
5-–9 June 2022, Oslo, Norway

VALIDATION OF THE TEMPERATURE HISTORY DURING EXTRUSION BASED ADDITIVE MANUFACTURING ECCOMAS CONGRESS 2022

Robert Hein[1] **and Felix Winkelmann**[2]

[1] German Aerospace Center (DLR)
Institute of Composite Structures and Adaptive Systems
Lilienthalplatz 7, 38108 Brunswick, Germany
e-mail: robert.hein@dlr.de, www.dlr.de

[2] German Aerospace Center (DLR)
Institute of Composite Structures and Adaptive Systems
Lilienthalplatz 7, 38108 Brunswick, Germany
e-mail: felix.winkelmann@dlr.de, www.dlr.de

Key words: Additive Manufacturing, Process simulation, Temperature measurement, Heat transfer, Crystallization kinetics

Abstract. Additive manufacturing (AM) is considered as a key technology for the efficient production of individualized components. The technique enables the tool-less production of complex geometries and designs that could not be realized cost-effectively with conventional manufacturing methods. The focus of this work is on the Fused Filament Fabrication (FFF), where a thermoplastic filament is extruded trough a nozzle. The material is deposited layer by layer until the final part is build. Thereby, high temperature gradients occur within the part when the hot material is deposited on the lower layers. During the printing process the lower layers are reheated several times so that the material properties are influenced even after the deposition has been made. The thermal history has major effects on crucial material properties such as the degree of crystallization or thermal and mechanical properties. An inadequate degree of crystallization influences both the structural properties such as the stiffness or the degree of bonding and the dimensional accuracy due to subsequent shrinkage effects. Additionally, the temperature gradients cause residual stresses which are partly relaxed to varying part deformations. The remaining stresses can lead to premature failures.
To achieve a high and repeatable part quality as well as a low scatter in the final part dimension an in-depth process understanding is required considering the underlying material-process-part-interactions. In order to analyse these complex multiphysical processes, manufacturing process simulations are a suitable method. A main requirement for the numerical analysis of AM processes is the calculation of the thermal history as accurately as possible. The objective of this work is, therefore, to evaluate the prediction accuracy of currently available AM process simulation tools. For this purpose, a gcode-based AM process simulation of a cuboid is performed in order to calculate the transient temperature fields using the Abaqus AM plug-in from Dassault Systèmes. The cuboid made of PETG is printed with a Prusa i3 MK3. In order to monitor the

temperature history during the printing process very thin thermocouples (0.25 mm) are integrated in the center of the part. The machine code (gcode) is transferred to the Abaqus and the transient temperature fields are predicted and compared to the measurements. The investigations have shown that commercial AM tools are capable to represent the fundamental physical processes. Furthermore, it has been shown that time-related differences occur due to deviations between the predefined gcode velocities and the real printer speeds caused by acceleration and deceleration effects of the printing head. For correct prediction of the temperature history the real printing speeds re required.

1 INTRODUCTION

In the context of rapidly rising raw material and energy costs, together with the need to meet the climate targets, there is a high demand for sustainable lightweight solutions. By reducing the moved weights and the associated energy consumption, resources can be saved significantly. Additive lightweight design, the combination of lightweight construction and additive manufacturing (AM), provides additional saving potential compared with conventional manufacturing methods because, in contrast to subtractive processes, the material is applied layer by layer so that only the required material is processed and the material waste is reduced to a minimum. The AM enables the tool-less production of complex bionic structures. Components can be manufactured on demand and on site, avoiding long supply chains and associated emissions as well as storage times.

The focus of this paper is on Fused Filament Fabrication (FFF). As shown in Figure 1, a thermoplastic filament is pushed through a heated nozzle to manufacture components layer-by-layer. In

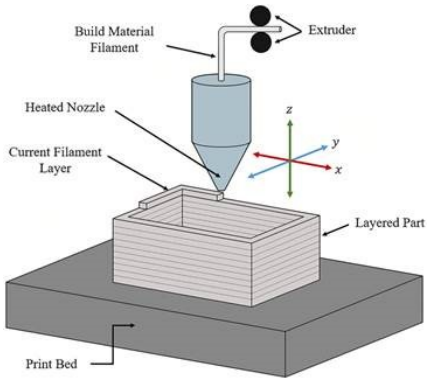

Figure 1: Schematic illustration of Fused Filament Fabrication Process [11]

contrast to metallic 3D printing, the exploitation of polymer based additive manufacturing for primary structures is still limited due to different causes. The final material and part properties are strongly affected by the temperature history during the printing process. In the case of semi-crystalline thermoplastics, the degree of crystallization is strongly affected by the cooling process. High cooling rates lead usually to a lower part crystallinity and lower cooling rates to a higher crystallinity. In the latter, the material is at elevated temperatures for longer periods of time resulting in more nucleation and growth. The crystallinity is related to the degree of struc-

tural order in a solid and influences the part properties significantly such as the bonding quality between adjacent beads or the mechanical and thermal properties. The hot extruded material is deposit on cooler filaments. Thereby, high temperature gradients arise resulting in residual stresses on micro, meso and macro scale. On macro scale the residual stresses are partly relaxed to part deformations such as warpage. On micro and meso scale, the remaining stresses can lead to premature failures. During the printing process the lower layers are reheated several times so that the material properties are influenced even after the material deposit. Furthermore, the thermal behavior is influenced due to anisotropic material behavior caused by the printing direction itself or potentially added reinforcements such as short or continuous fibers. Furthermore, different infill pattern and densities or multi-materials affect the thermal and mechanical part properties.

Because of the many influencing parameters, it is very challenging to derive the right process parameters. Currently, the derived printing parameters are based on data sheets from the material manufacturer or supplier and on printing tests. This iterative trial-and-error approach can be very time-intensive and costly, especially when high performance materials such as PEEK or PAEK are utilized which are extruded at high temperatures. In order to reduce development costs and to speed-up the engineering times, manufacturing process simulation of the printing process are more and more applied. This allows the analysis of the effect of printing parameters on the material and part properties and enables an in-depth process understanding. Within the recent years, different commercial simulation tools such as Abaqus AM [13], Ansys Additve [2], Digimat AM [6] and many more were developed. In fact, the tools are available but there is a lack of validation use-cases in order to evaluate the prediction accuracy. Therefore, the objective of this work is to evaluate the prediction accuracy of commercial tools with respect to the thermal history. For this purpose, the finite element solver of Abaqus with the Additive Manufacturing (AM) plug-in is used. The thermal history of a simple cuboid structure is measured during the printing process by means of a embedded thin thermo-couple. Afterwards the printing process is simulated and the measured and simulated temperature history are compared. Deviations in the results are discussed and the causes are investigated in further experiments.

2 TEMPERATURE MEASUREMENT DURING THE PRINTING PROCESS

In order to investigate the thermal history a cuboid with the dimensions 100 mm × 25 mm × 10 mm (length x width x height) is printed (see Figure 2, left). For temperature measurement a small cavity of 0.3 mm × 0.3 mm is introduced in the center of the part in order to place a thermocouple (type k, inconel) with a diameter of 0.25 mm. A Prusa MKi3 [9] is used as printer. It has an open build chamber which enables the integration of additional sensors in contrast to the most printers with a closed heated chamber. PETG is used as thermoplastic material. The extrusion temperature is set to 245 °C and the print bed temperature is set to 80 °C according to the material data sheet [10]. The cuboid is manufactured with 100 % infill. Styropor plates with a thickness of 10 mm are distributed around the printer in order to avoid external heat convection.

Figure 3 shows the obtained temperature history in the center of the cuboid as well as of the base plate. The measured base plate temperature is with 66 °C lower than the predefined temperature

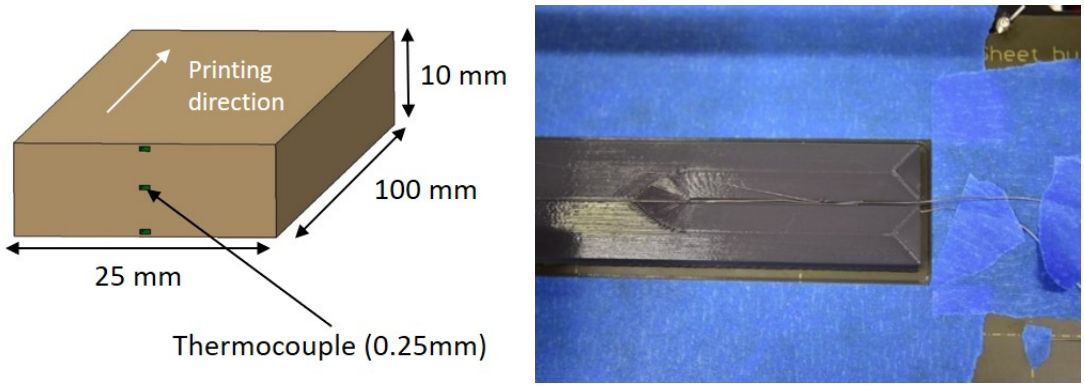

Figure 2: **Left:** Used test structure for temperature measurements, **Right:** Embedded thermocouple

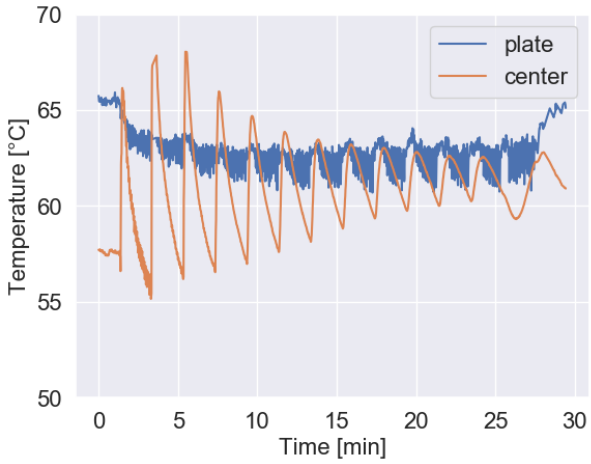

Figure 3: Obtained temperatures for base plate and part center

of 80 °C because of the magnetic print pad between the heating plate and the sensor. After starting the printing process the temperature at the base plate decreases to ≈63 °C because of the movement of the plate. In order to place the thermocouple, the printing process is paused just before the cavity is almost completed (see Figure 2, right). After installing of the sensor the printing process is proceeded. Every time when a new layer is deposit a temperature peak can be observed in Figure 3. The temperature peaks increases first because of changed thermal boundary conditions when the cavity is closed. The maximum measured peak temperature is about 68 °C. With proceeding printing time the temperature peaks decrease because of the increasing distance between newly deposit layers and the sensor position.

3 FFF PROCESS SIMULATION

The process simulation of extrusion based additive manufacturing is a challenging task. The phenomena occur over multiple length scales. The extruded filament has a typical cross-section of between 0.1 mm to 0.5 mm for small-scale printers with a building chamber size of

25 mm × 25 mm × 30 mm. Large-scale printers such as the Big Area Additive Manufacturing (BAAM) printer by Cincinnati Lab have a building chamber of 6096 mm × 2286 mm × 1829 mm [5] and deposit filaments with 8 mm in diameter. So, there is a large ratio between one single layer and the final part dimensions. Depending on the research question, a very high resolution of the model is probably needed resulting in large and computational intensive models. Furthermore, the phenomena occur over multiple time scales. The cooling process of a newly deposit filament take place within a few seconds or less but the building time of the entire part can be take several hours or days. Additionally, the material behavior is very complex. The material goes from a liquid phase over to a temperature-dependent viscoelastic solid with glass transition and crystallization in the case of partly-crystallized thermoplastics.

Recently, gcode based finite element simulation methods were developed from commercial software supplier in order to capture the mentioned phenomena. The basic concept shall be briefly introduced using the AM Plug-in of Abaqus as an example. As demonstrated in Figure 4, the CAD geometry is meshed with hexaeder or voxel elements in a first step. As second, the gcode

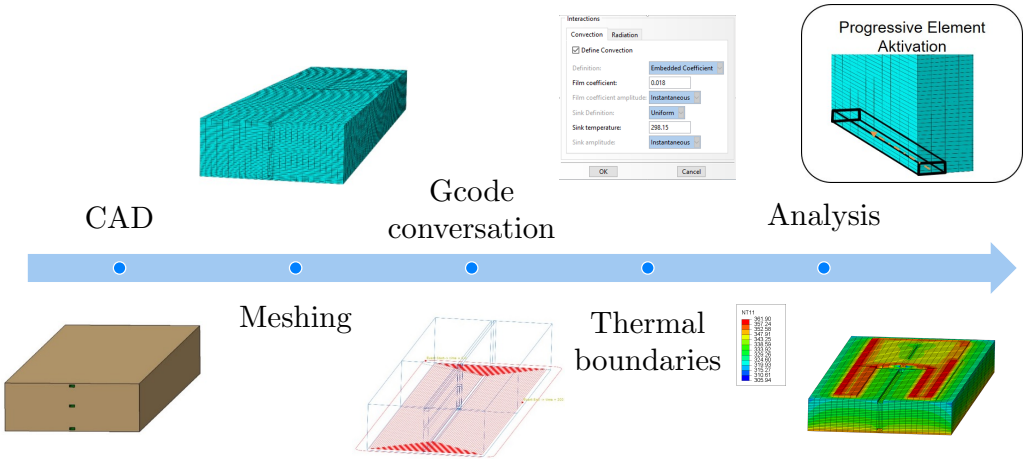

Figure 4: Basic workflow for a FFF process simulation

coming from the slicer software need to be converted in an Abaqus-specific format, the so called event series. This format describes the position of the printing head in dependency on the time. Other software vendors such as Ansys or Digimat are working directly with the gcode. After assigning of the thermal boundary conditions such as the base plate temperature, chamber temperature, extrusion temperature, heat convection and radiation, the thermal analysis is performed. Thereby, a progressive element activation method is applied. This is an geometry-based tool which intersects the event series with the finite elements and activates the elements layer-by-layer according to the gcode. The evolving element faces for heat convection and radiation

are updated automatically. This technique is more efficient than the classical element birth and death technique.

4 COMPARISON OF THE MEASURED AND SIMULATED TEMPERATURES

A process simulation of the printing process is conducted applying the methodology introduced in the previous section. The assigned boundary conditions are shown in Figure 5. For the

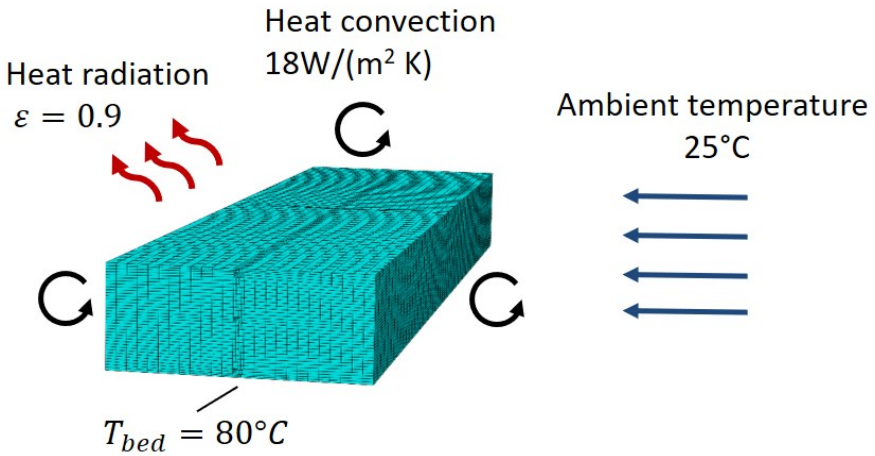

Figure 5: Asssigned thermal boundary conditions

heat radiation a heat emissivity of 0.9 is applied based on thermo-camera measurements (FLIR A65 FOV90). Therefore, the surface temperature of the cuboid is measured with a thermocouple and the emissivity is adjusted till the thermo-camera measurements matches the temperatures of the thermocouple. A initial temperature of 245 °C is assigned to the elements according to the extrusion temperature. This means, that the elements are activated with the assigned initial temperature and the new thermal equilibrium is calculated for each increment. A heat convection coefficient of 18 $\mathrm{W\,m^{-2}\,K^{-1}}$ is assumed based on literature data [4]. The ambient temperature is set to 25 °C.

Figure 6 shows the comparison of the measured (Thermocouple (TC) center) and simulated temperature in the cavity. The graphs reveal that the general thermal behavior is qualitatively well approximated by the simulation. The predicted temperature peaks are higher than the measured temperature peaks. The differences can be reduced by optimized boundary conditions in the simulation, e.g. by assigning a printing height dependent heat convection and temperature-dependent conductivity. Further, the calculated temperature values vary also in dependency on the selected finite element node. Additionally, further experiments with respect to the diameter of the thermocouples have revealed that the measured peak values strongly dependent on the used thermo-couple diameter. The absolute peak values are attenuated because of the thermal inertia of the thermo-couple. In fact, a thinner thermo-couples, e.g. 0.08 mm, result into higher peak values so that simulated and measured values converge further.

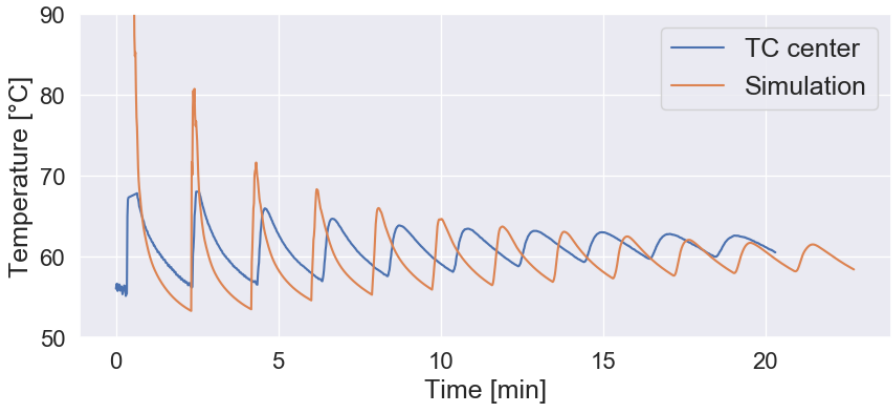

Figure 6: Comparison of the measured and simulated temperature in the cavity

The most important point in this graph, however, is the delay between the measurement and the simulation despite of the identical gcode. This leads to an inaccurate prediction of the temperature history. The simulated process is faster than the real process which should not be occur. This aspect is investigated in the next section in more detail.

5 ANALYSES OF THE PRINTING HEAD KINEMATICS

As cause for the time delay between the simulation and the measurements, it is assumed that the real printing speed deviates from the planned speed. In order to investigate this aspect, the kinematic behavior of the printing head is studied using a laser triangulation. The experimental set-up is shown in Figure 7. The printing head is moved horizontally with different predefined velocities and the displacement is monitored in dependency on the time. Figure 8 shows exemplary the measurement result for a printing speed of $1000\,\mathrm{mm\,min^{-1}}$. Based on the upper and lower peak values (red dots in Figure 8) the velocity v of each movement is calculated with:

$$v = \frac{s}{t} \tag{1}$$

where s and t are the displacement and the time for one partial distance. Finally, the mean velocity is calculated. This procedure is repeated for different velocities. The obtained results are summarized in Table 1. The table reveals that with increasing velocity the deviations between the predefined and real velocities increase. The cause for the deviations are the acceleration and deceleration of the printing head. Therefore it should be taken into account that the predefined gcode velocities can differ from the real printer speed resulting in differences between simulation and measurement results. For precise prediction of temperatures, it is important to have the real printer speed. These are provided, for example, by modern CNC based control systems such as the CNC Sinumerik from Siemens [12].

6 APPLICATION: CALCULATION OF THE CRYSTALLIZATION KINETICS

For semi-crystallized thermoplastics the degree of crystallization has an crucial impact on the mechanical properties. The crystals are developing mainly during the cooling phase when

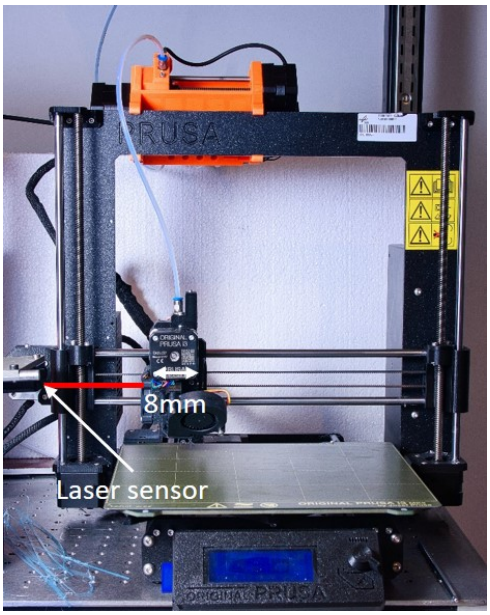

Figure 7: Experimental set-up to analyses the kinematic behavior of the print head

Table 1: Comparison of the planned and real printing speeds

Velocity [mm/min]	Target [$\mathrm{mm\,s^{-1}}$]	Real [$\mathrm{mm\,s^{-1}}$]
F1000	16.66	16.23
F2000	33.33	29.91
F3000	50.00	37.21
F4000	66.66	45.31
F5000	83.30	48.02
F7000	116.67	50.41

the part temperature is between the melting temperature and the glass transition temperature. During the printing process underlying layers are reheated again when a new layers is deposit. Thereby, the degree of crystallization of both the underlying layers and the new layer are affected. Thus, it is important to know the temperature history in order to evaluate the current part crystallinity and the associated part quality.
The degree of crystallization is usually determined via Differential Scanning Calomitry (DSC) measurements. For lower cooling rates, which occur e.g. at large scale printing, conventional DSC measurements with cooling rates up to $100\,\mathrm{K\,min^{-1}}$ are sufficient. For smaller nozzles, e.g 0.3 mm or smaller, high cooling rates up to $3000\,\mathrm{K\,min^{-1}}$ can be observed. To capture the crystallization kinetics for high cooling rates Flash-DSC measurements are probably necessary [14].
For modeling of the crystallization kinetics two principal approaches exist in literature: the mechanistic approach and the phenomenological approach [1]. At the mechanistic approach the

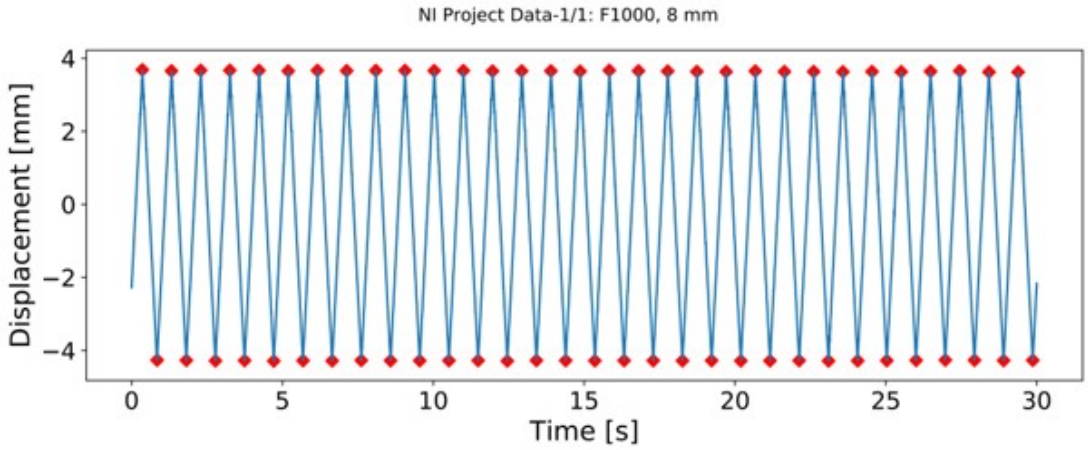

Figure 8: Measured displacements of the printing head

polymerization of the particular polymer chains is modeled. The reactions show often a complex nature, e.g. the ring opening, and require large computational times [7]. Therefore, phenomenological approaches are mostly applied. Thereby, the crystallization process is observed, e.g. by DSC measurements, and the behavior is approximated with a mathematical expression. The unknowns in the equations are fitted to the measurements. The obtained equation can be integrated into commercial finite element codes by means of user subroutines.
Figure 9 shows the principal workflow for the consideration of crystallization kinetics. Starting point are DSC or Flash-DSC measurements at different cooling rate. A proper material model

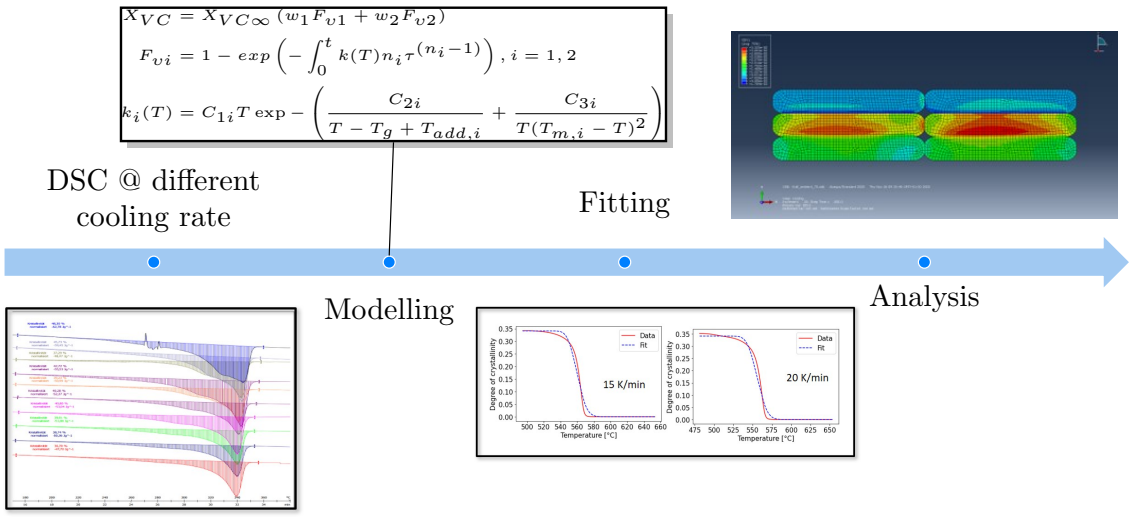

Figure 9: Modelling of the crystallization behavior and its integration in Abaqus

need to be chosen in the next step. In this case a dual kinetics model proposed from Velisaris et al. [15] is employed. The approach is based on the Avrami approach [3] and considers nucleation and growth processes. Another widely used model is the model proposed by Nakamura [8]. Next, the model parameters (13 for the model from Velisaris et al.) need to be fitted to DSC/Flash DSC measurements. Therefore, a python-based differential evolution algorithm is utilized to find the global optimum. In order to calculate the degree of the crystallization distribution within an arbitrary geometry, the equation can be integrated in commercial software applications by means of user subroutines. The subroutine is called during each iteration and calculates the local crystallinity in dependency on the current temperature and time. This is repeated for all integration points. Coupled with the introduced AM process simulation the part crystallinity can be calculated considering the temperature history.

7 CONCLUSIONS

It has been shown that commercial FEM software vendors provide efficient tools for AM simulations capturing the underlying physics. The challenge is to apply appropriate boundary conditions, interactions and material models. The temperature measurements during the printing have shown that the predefined gcode velocities can be deviate from the real printer speeds resulting in differences between the simulated and measured temperature history. The deviations increase with increasing printing speed and decreasing path lengths. In these cases acceleration and deceleration effects of the printing head are getting more dominant. For the purpose of validation, the real printing speeds should be considered. It is worth to mention that for small desktop printer high cooling rates up to $3000\,\mathrm{K\,min^{-1}}$ occur, especially when high-temperature thermoplastic materials are used. The crystallization kinetics can potentially not be measured properly with conventional DSC measurements and Flash-DSC measurements should be considered. Furthermore, it has been shown that the AM process simulation coupled with a crystallization model enables the calculation of the part crystallinity under consideration of the temperature history. This allows the evaluation of the part quality and the derivation of optimal process parameters.

ACKNOWLEDGMENT

The authors gratefully acknowledge the Technology Marketing of the German Aerospace Center (DLR) for the financial support within the Innovation Lab EmpowerAX (EmpowerAX).

REFERENCES

[1] Ageyeva, Sibikin, and Kovács. “A Review of Thermoplastic Resin Transfer Molding: Process Modeling and Simulation”. In: *Polymers* 11.10 (Sept. 2019), p. 1555. ISSN: 2073-4360. DOI: 10.3390/polym11101555. URL: https://www.mdpi.com/2073-4360/11/10/1555.

[2] Ansys. *Ansys Additive Solutions*. 2022. URL: https://www.ansys.com/products/additive.

[3] Melvin Avrami. “Kinetics of Phase Change. I General Theory”. In: *The Journal of Chemical Physics* 7.12 (Dec. 1939), pp. 1103–1112. ISSN: 0021-9606. DOI: 10.1063/1.1750380. URL: http://aip.scitation.org/doi/10.1063/1.1750380.

[4] Bastian Brenken. "EXTRUSION DEPOSITION ADDITIVE MANUFACTURING OF FIBER REINFORCED SEMI-CRYSTALLINE POLYMERS by School of Aeronautics & Astronautics". PhD thesis. PURDUE UNIVERSITY, 2017, p. 248.

[5] Phillip Chesser et al. "Extrusion control for high quality printing on Big Area Additive Manufacturing (BAAM) systems". In: *Additive Manufacturing* 28 (Aug. 2019), pp. 445–455. ISSN: 22148604. DOI: 10.1016/j.addma.2019.05.020. URL: https://linkinghub.elsevier.com/retrieve/pii/S2214860418307000.

[6] Hexagon. *Digimat Solutions*. 2022. URL: https://www.e-xstream.com/product/digimat-am.

[7] D. J. Lin, J. M. Ottino, and E. L. Thomas. "A kinetic study of the activated anionic polymerization of ?-caprolactam". In: *Polymer Engineering and Science* 25.18 (Dec. 1985), pp. 1155–1163. ISSN: 0032-3888. DOI: 10.1002/pen.760251808. URL: https://onlinelibrary.wiley.com/doi/10.1002/pen.760251808.

[8] K. Nakamura et al. "Some aspects of nonisothermal crystallization of polymers. I. Relationship between crystallization temperature, crystallinity, and cooling conditions". In: *Journal of Applied Polymer Science* 16.5 (May 1972), pp. 1077–1091. ISSN: 00218995. DOI: 10.1002/app.1972.070160503. URL: https://onlinelibrary.wiley.com/doi/10.1002/app.1972.070160503.

[9] Prusament. *Original Prusa i3 MK3*. 2022. URL: https://www.prusa3d.com/.

[10] Prusament. *TECHNICAL DATA SHEET: Prusament PETG by Prusa Polymers*. 2022. URL: https://prusament.com/media/2018/09/Prusament_techsheet_PETG-1-1.pdf.

[11] J Shah et al. "Large-scale 3D printers for additive manufacturing: design considerations and challenges". In: *The International Journal of Advanced Manufacturing Technology* 104.9-12 (Oct. 2019), pp. 3679–3693. ISSN: 0268-3768. DOI: 10.1007/s00170-019-04074-6. URL: https://doi.org/10.1007/s00170-019-04074-6%20http://link.springer.com/10.1007/s00170-019-04074-6.

[12] Siemens. *SINUMERIK CNC systems*. 2022. URL: https://new.siemens.com/global/en/products/automation/systems/cnc-sinumerik/automation-systems.html.

[13] Dassault Systems. *PRINT TO PERFORM: SIMULATION FOR ADDITIVE MANUFACTURING*. 2022. URL: https://www.3ds.com/products-services/simulia/trends/digital-additive-manufacturing/.

[14] Xavier Tardif et al. "Experimental study of crystallization of PolyEtherEtherKetone (PEEK) over a large temperature range using a nano-calorimeter". In: *Polymer Testing* 36 (June 2014), pp. 10–19. ISSN: 01429418. DOI: 10.1016/j.polymertesting.2014.03.013. URL: https://linkinghub.elsevier.com/retrieve/pii/S0142941814000713.

[15] Chris N Velisaris and James C Seferis. "Crystallization Kinetics of Polyetheretherketone (PEEK)". In: *Polymer Engineering and Science* 26.22 (Dec. 1986), pp. 1574–1581. ISSN: 0032-3888. DOI: 10.1002/pen.760262208. URL: http://dx.doi.org/10.1002/pen.760262208%20http://doi.wiley.com/10.1002/pen.760262208%20https://doi.org/10.1002%2Fpen.760262208.